Physical characteristics of nanoparticles emitted during drilling of silica based polyamide 6 nanocomposites

Sophia Sachse[1], Francesco Silva[1], Adeel Irfan[2], Huijun Zhu[2], Krzysztof Pielichowski [3], Agnieszka Leszczynska [3], Maria Blazquez [4], Olga Kazmina [5], Oleksandr Kuzmenko [6] and James Njuguna[1]*

[1] Department of Environmental Science and Technology, Cranfield University, Bedfordshire MK43 0AL, UK
[2] Cranfield Health, Cranfield University, Bedfordshire MK43 0AL, UK
[3] Department of Technology of Polymers, Cracow University of Technology, ul. Warszawska 24, 31-155 Krakow, Poland
[4] Ekotek Ingenieri y Consultoria Medioambiental, Erandio, Bizkaia, 48950 Spain
[5] Department of Silicate Technology and Nanotechnology, Tomsk Polytechnic University,634050 Tomsk, Russia
[6] Palladin Institute of Biochemistry, National Academy of Sciences of Ukraine (NASU), Kiev, 01601 Ukraine

E-mail: `j.njuguna@cranfield.ac.uk` (*Corresponded Author:)

Abstract.
During the past decade, polymer nanocomposites have emerged as a novel and rapidly developing class of materials and attracted considerable investment in research and development worldwide. However, there is currently a lack of information available in the literature on the emission rates of particles from these material. In this study, real-time characterization of the size distribution and number concentration of sub-micrometer-sized particles (5.6-512 nm) emitted from polyamide 6 nanocomposites during mechanical drilling was made. For the first time, four different silica based filler of commonly use were assessed. Further, the respective emission rates were determined based on the particle population and the time. The measurements showed that the particle emission rates ranged from 1.16E+07 (min^{-1}) to 1.03E+09 (min^{-1}) and that the peak diameters varied from 29.6 to 75.1 nm. Airborne particles in the nanometer range (11.1-46.8 nm), in the ultrafine range (51.3-101.1 nm) and in the accumulation mode range (111.9-521 nm) accounted for 34.1% to 76.6%, 8.3% to 47% and 4.1% to 24.2% of the total emission rates, respectively, depending on the type of filler. Additionally, deposited particles were sampled and characterized, to explore any possible correlation between deposited and airborne particles. The result clearly showed that with increasing airborne particle concentration the deposit particle concentration decreased and vice verse.

1. Introduction
Polymer nano-composites have proven huge potential in both mechanical and thermal application J. et al. [2010], Njuguna et al. [2011]. The global consumption of nanocomposites is estimated to exceed 214,081 metric tons and 1.38 billion USD, by 2014BCCResearch [2010]. Of which the consumption of clay-based polymer nanocomposites will increase to 181,094 metric

tons and 692.3 million USD by 2014. For example, one of the leading automotive manufacturers is using 300000 kg of nanoclay composites annually for various automotive exterior part/panel applications at presentBCCResearch [2010]. However, only little attention has been payed to the end user contact with nanocomposites by science and regulators. Despite the worst case scenario of a nanocomposite being the encounter with a do it yourself (DIY) worker C. et al. [2010]. The DIY-worker's personal protection in general consist of an low-cost filter mask, which might be inadequate for protection against nanoparticle particles inhalation. In the car tuning scene, a common way to reduce the weight of a car is the drilling of small holes. Further other car modifications e.g. integration of a new stereo, system or body kit are imaginable and will involve drilling into those nanocomposites Scott J. [2006]. However, during drilling, shear forces may detach free nanofillers as ultrafine airborne particles. Due to their size, these particles are able to remain airborne for a long period M. [2004] and are suspected to enter the human cells more easily via respiratory, dermal or oral absorptionA. et al. [2011]. The high biological activity can be explained by the large surface-to-volume ratio; hence many types of nanoparticles have shown toxic impact A. et al. [2011], L. [2004], G. [2010], D. et al. [2011]. In the current work, airborne particles emitted by silica filled polyamide 6 nanocomposites by mechanical drilling were investigated in a controlled environment. The particle number concentration and the size distribution were measured continuously in real time using a particle sizer. In addition, the particles emission rates were evaluated as this information could be useful in assessing the resulting human exposure.

2. Methodology
2.1. Materials
Polyamide 6 (Tarnamid T30, Azoty Tarnow, Poland) was used as matrix material for all composites. As fillers the following materials were utilised (5wt.%); montmorillonite layered nanosilicates (Laviosa/Dellite 43B), nanosilica (Degussa/AEROSIL 200), foam-glass-crystal-materials (Produced by Tomsk Polytechnic University) and glass fibres (Taiwan glass Industry Co./ 473H).

2.2. Nanocomposite manufacturing
A twin-screw extruder (ZMK/116/10, ZAMAK - Cable Machinery Plant, Poland) was utilized to compound the PA6 matrix and 5 wt.% of montmorillonite (MMT), nanosilica (SiO_2) and foam-glass-crystal-materials (FGC). Extruder screws diameter was 24 mm, had a length/diameter ratio of 32 and consisted of 6 barrel zones. A conventional screw configuration for material compounding was. The screws were equipped with two high-shearing zones in a second and fifth zone. Single-screw extruder (ZMK/117/10, ZAMAK Zaklad Maszyn, Poland) with a length/diameter ratio of 25 and a screw diameter of 25 mm was used for manufacturing of the PA6-glass fiber (PA6/GF) granulate. The single-screw extruder provided effective homogenization of classic fillers without changing the geometry of glass fibres. The panels were prepared by compression moulding technique. The mould temperature was kept at 250°C over the compression time of 5 min. Due to the high dimensions (100x100x10 mm^3) of the panels, cooling of polymer melt was completed in the mould in order to avoid warping.Additional unreinforced PA6 panels have been manufactured in the same way as the reinforced ones, as reference material

2.3. Measurement of number concentration and size distribution
To characterize the physical properties of particles generated during drilling, composite panels were fixed in a chamber, with dimensions 68.58cm (width) x 33.02cm(depth) x 55.88cm(height) as illustrated in Fig. 1. The particle emissions were measured using a Condensation Particle Counter "CPC" 5.403 with Classifier "Vienna"-DMA 5.5-U (SMPS+C, Grimm Aerosol,

Germany). SMPS+C measured sub-micrometer particles generated during drilling process over a particle size range of 5.6-1083 nm and a particle size resolution of 32 channels in total. An angle drill (Makita BDA351Z 18V LXT Angle Drill) was used for drilling with a maximum speed of 1800 min^{-1}, adapted with a conventional drill bit of 10mm diameter. Prior to measurements, the chamber was purged with laboratory air for about 20 min. Each sampling cycle comprised a 60 min background air monitoring in the chamber, 14 min. of active drilling, and a 60 min postdrilling period. The experiment was repeated 3 times for each material composition. A total of about 2000 to 3000 data sets were collected for each particular sequence.
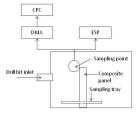

Figure 1: Apparatus and setup for the chamber experiments

2.4. Determination of emission rates
The emission rates of particles of different sizes were determined from the number concentration and size distribution data based on a single compartment population balance model. Liu et al. W. et al. [2003] used a mass balance model to estimate emission rates of particles based on mass concentrations. As reported by See et al. S.W. et al. [2007], the mass balance model calculation can also be used to estimate the particle emission rate based on particle population. Basic assumptions for this model were made as followed: a) particles are assumed to be perfect spheres with a constant density; b) background concentration is zero; b) particle concentrations are homogeneous within the chamber; and d) emission rate and decay rate of the particles remain constant throughout the entire period of generation.

The respective removal rates k_x (min^{-1}) of a particle size x were evaluated using the following equation:

$$k_x = \frac{ln(C_x/C_{max;x})}{T-t}; \quad \text{for } t \geq T \tag{1}$$

where C_x (cm^{-3}) represents the number concentration of particles of size x at time t (min), while $C_{max;x}$ (cm^{-3}) represents the maximum concentration of particles of size x which at the time T (min). The background concentration of particles, averaged over the 60 min pre-burning interval, was subtracted from the concentration readings to compute C_x (cm^{-3}) and $C_{max;x}$.

After calculating the removal rates k_x, the emission rate of particles of size x, P_x (min^{-1}) in the chamber volume V ($1,26540 \times 10^5$ cm^{-3}), was calculated from:

$$P_x = \frac{VC_x k_x}{1-e^{k_x t}}; \quad \text{for } 0 \leq t \leq T \tag{2}$$

3. Results and Discussion
3.1. Sequential alteration of number concentration and size distribution
The sequential alteration of the total number concentration of particles for a typical sampling cycle is shown in Fig. 2. It consists of a 60-min background measurement ($t \geq T$), the 15min drilling period($0 \leq t \leq T$), and a 120-min post-drilling period ($t \geq T$). Figure 2, shows that the total number concentration of particles was essentially constant with an

average of 1000 particles/cm^{-3} before the drilling process. As soon as drilling started inside the experimental chamber, the number concentration increased rapidly. The maximum number concentration, C$_{max}$, was reached at time T. Subsequently, the particle decay was observed with the concentration falling back to the original background level approximately after a post drilling period of 2h. In significant research studies I.K et al. [2009], K. et al. [2009], W.-C. [1997], R. et al. [2007] the influence of the machining engines as "background noises" on the results has been reported. As the drilling was conducting in a controlled environment, the influence of the machining engine could be reduced to a minimum, as shown in figure 2. Highest C$_{max}$ could be measured for the nanosilica filled composites. Wohlleben et al. W. et al. [2011] reported that, while comparing nanocomposites with their reference materials without nanofillers, the differences are insignificant in the number concentrations of aerosols during normal abrasion use. This statement can not be substantiated, as the results strongly suggest that the integration of nanofillers changes the material behavior and thus the amount of particle emitted during drilling.
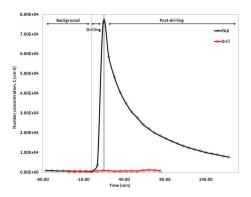

Figure 2: Sequential alteration of number concentration of a typical sampling cycle

Diffusion, gravitational deposition, convection, impaction, and coagulation are some of the complex processes which influence formation and removal of particles in the chamber. Removal of small particles is primary dominated by diffusion while larger particles are mainly affected by gravitation. During diffusion, small particles collide with one another and form larger particles Grassian V. H. [2008]. This process is known as coagulation and strongly depended on particle size and concentration. While the coagulation rate of a simple monodisperse particle population can be calculated using equation 3 Hinds [1982],

$$\frac{dN}{dt} = KN^2 \qquad (3)$$

where N is particle number concentration and K is the coagulation coefficient. Based on this equation, the coagulation rate is directly proportional to the diffusion coefficient and particle size and therefore decreases with particle size. An indication of the coagulation rate can be identified by the half-life of an individual particle, which is introduced into an atmosphere embracing a defined concentration of such particles Grassian V. H. [2008]. However, according to Hinds Hinds [1982] coagulation can be neglected for laboratory experiments if the particle concentration is less the $1x10^{12}$m^{-3}. As the maximum concentration measured in this study did not exceed $1.7x10^{11}$m^{-3}, coagulation was neglected.

The particle size distributions of drilling into different material systems is shown in Figure 3. The plots reflected particle size distributions at T, the time particle concentration reached it maximum and drilling was terminated. The plots presented the normalized distribution with ΔN/Δlnd_p versus the particle diameter d$_p$, where ΔN is the concentration of particles within

a specified size interval and $\Delta \ln d_p$ is the difference in the natural logarithm of the largest and smallest particle sizes of that interval. From visual inspection of the graph, it could be noted that from different composite distinct modal diameters were obtained and that they appear to be dependent of the filler used. A major difference in peaks could be observed between the different fillers. The peaks varied from 29.6 nm for the nanosilica composite to 75.1nm for neat PA6. This showed that integration of nanofillers changes the physical properties of the emitted particles. This results contradict with the results obtained in some recent studies I.K et al. [2009], W. et al. [2011], M. et al. [2009]. For example, Wohlleben et al. W. et al. [2011] reported, while comparing nanocomposites with their reference materials without nanofillers, that both the differences in the number concentrations and in the actual size distribution of aerosols during normal abrasion use, were insignificant. However, these studies dealt with abrasion and sanding of surfaces and composites. The difference in mechanical processing could explain the alterations in the obtained results.
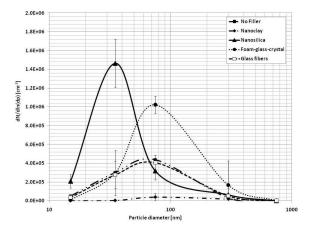

Figure 3: Normalized particle size distributions at time T

To support the results obtained by SMPS+C particles were sampled via an electrostatic precipitator (ESP, Grimm Aerosols, Germany) and subjected to JFEI XL30 field emission scanning electron microscope. The scanning electron micrographs of the particles generated during drilling of different composites are represented in Figure 4. Micrographs of the particles generated from PA6/FGC (Fig. 4a)., PA6/SiO$_2$ (Fig. 4b)and the neat PA6 (Fig. 4e) composites showed very similar structures of coagulated particle. Smaller generated particles (20-50nm), coagulated to larger particles 150nm, which were then sampled by ESP over a time frame of 2h. According to the literature Grassian V. H. [2008], the half time of particles in the size range of 10-200nm in the measured concentration would be between 16-83 min, therefore coagulates of particles are natural for such a long sampling period. The SEM image of the generated particles obtained from drilling of the glass fiber panels (Fig. 4d), showed agglomeration of larger particles. Furthermore the particles seem to be glass fibers debris, as the structure is very similar to structure seen in the bulk panels. Visual investigation of the particles obtained from drilling of the nanoclay composites (Fig. 4c)were scattered over the sampling plate and no coagulation could be found. This could be explained by the low particle concentration that was measured for this composite.

3.2. Emission rates of different composite materials
The emission rates of size-distributed particles from different composites were determinate using Eq. 2, after taking into account the removal rates of particles of different sizes from Eq. 1. The stacked column charts of Figure 5 shows the number of particles that were emitted per minute

(a) PA6/foam-glass-crystal   (b) PA6/nanosilica   (c) PA6/nanoclay
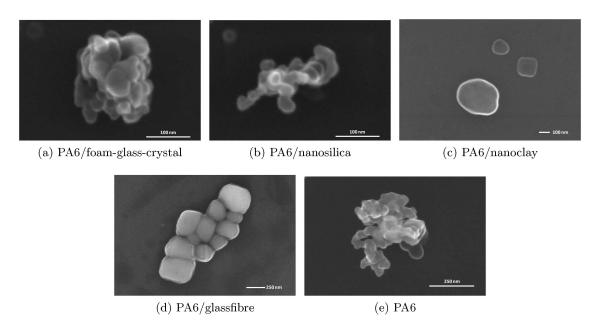
(d) PA6/glassfibre   (e) PA6

Figure 4: SEM micrographs of generated particles collected by ESP

during drilling of the composite materials. The error bars represent the standard deviation associated with the total emission rate of 11.1-521nm particles resulting from the three replicate measurements. Table **??** represents the total emission rates for the different composite materials. Lowest emission rates could be calculated for the nanoclay filled composites, followed by the neat PA6 panel. Highest emission was calculated for the nanosilica filled material. However, while comparing the percentage of the individual size intervals on the total emission, it could be seen that for all materials (beside nanoclay) the majority of particles, 45-59%, were in the size range of 22.6-42.6 nm (Figure 5). Further the un-filled material emitted the largest quantity (25%) of particles larger than 100nm. The emission rate increased by 56 times for the nanosilica filler and between 20-45 times for the glass fibre and foam-glass crystal filler. Interestingly, integration of nanoclay into the PA6 matrix reduced particle emission during drilling by 1.5 times. It is likely that the presence of nanoclay in some way retains the formation of high quantity of airborne particles. This could be caused due to modification of the nanoclay prior integration of the matrix, however other reason could be plausible e.g. shape of the nanoclay filler and integration mechanism into the matrix (intercalation/exfoliation) A. et al. [2007a,b].

4. Conclusion
Physical characterization of the number concentration and size distribution of sub-micron particles from 5.6 to 512nm was carried out, for the first time, for different silica based nanocomposites. Two kind of nanosilica fillers (nanoclay, nanocilica) and two kind of macro silica filler (glass fibres and foam-glass crystal) were successfully integrated into a PA6 matrix. Based on size-resolved particulate emission rates from various silica based composites during mechanical drilling process were evaluated. In general, nano and ultrafine airborne particles were emitted from all investigated materials, even the non reinforced polymer. However emission increased by 56 times for the nanosilica filler and between 20-45 times for the glass fiber and foam-glass crystal filler. Interestingly, integration of nanoclay into the PA6 matrix reduced particle emission during drilling by 1.5 times. However, the characterisation of deposited particles showed exactly the opposite particle behavior, as with decreasing airborne particle concentration the deposit particle concentration increased and vice verse. This study has certainly shown that the integration of

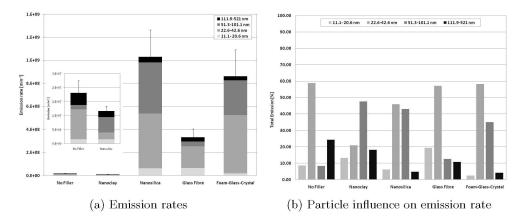(a) Emission rates   (b) Particle influence on emission rate

Figure 5: Emission rates of particles for different composites

nanofillers into polymeric matrix, changes the behaviour of the composite material in terms of particle emissions. Therefore, future work will involve a series of comprehensive chemical characterization of size-distributed particles released during drilling of nanocomposites to make a better assessment of public health outcomes due to exposure.

5. Acknowledgment

References
Njuguna J., Sachse S., Ifran A., Zhu H., Michalowski S., and Pielichowski K. Nanoparticles released from structural nano-enhanced products following mechanical loading at low velocity impacts: A case study on structural polyurethane nanoreinforced foams. In *4th International Seminar on Modern Polymeric Materials for Environmental Applications*, volume 4, pages 247–254, 2010.

J. Njuguna, Silva F., and Sachse S. *Nanocomposites for Vehicle Structural Applications, Nanofibers - Production, Properties and Functional Applications*, chapter 19, pages 402–434. InTech, 2011.

BCCResearch. Nanotechnology - nanocomposites, nanoparticles, nanoclays, and nanotubes. Technical Report NAN021D, BCC Research, 2010.

Som C., Berges M., Chaudhry Q., Dusinska M., Fernandes T.F., Olsen S.I., and Nowack B. The importance of life cycle concepts for the development of safe nanoproducts. *Toxicology.*, 269: 160–9, 2010.

and Scott J. *How to Rebuild and Modify Your Muscle Car.* MotorBooks International, 2006.

Harrison R. M. Review: Key pollutants - airborne particles. *Sci. Total Environ.*, 334:3–8, 2004.

Sotiriou G. A., Diaz E., Long M. S., Godleski J., Brain J., Pratsinis S. E., and Demokritou. P. A novel platform for pulmonary and cardiovascular toxicological characterization of inhaled engineered nanomaterials. *Nanotoxicology*, 0(0):1–11, 2011.

Dreher K. L. Health and environmental impact of nanotechnology: Toxicological assessment of manufactured nanoparticles. *Toxicol. Sci.*, 77:3–5, 2004.

Oberdrster G. Safety assessment for nanotechnology and nanomedicine: concepts of nanotoxicology. *Journal of Internal Medicine*, 267(1):89–105, 2010. ISSN 1365-2796.

Maynard A. D., Warheit D. B., and Philbert M. A. The new toxicology of sophisticated materials: Nanotoxicology and beyond. *Toxicological Sciences*, 120(suppl 1):S109–S129, 2011.

Liu W., Zhang J., Hashim J.H., Jalaludin J., Hashim Z., and Goldstein B. D. Mosquito coil emissions and health implications. *Environ. Health Perspect.*, 111:1454–1460, 2003.

See S.W., Balasubramanian R., and Joshi U.M. Physical characteristics of nanoparticles emitted from incense smoke. *Science and Technology of Advanced Materials*, 8(1-2):25, 2007.

Koponen I.K, Jensen K.A., and Schneider T. Sanding dust from nanoparticle-containing paints: Physical characterisation. *Journal of Physics: Conference Series*, 151(1):012048, 2009.

Jensen K., Koponen I., Clausen P., and Schneider T. Dustiness behaviour of loose and compacted bentonite and organoclay powders: What is the difference in exposure risk? *Journal of Nanoparticle Research*, 11:133–146, 2009. ISSN 1388-0764.

Chen W.-C. Some experimental investigations in the drilling of carbon fiber-reinforced plastic (cfrp) composite laminates. *International Journal of Machine Tools and Manufacture*, 37(8): 1097–1108, 1997. cited By (since 1996) 71.

Khettabi R., Songmene V., and Masounave J. Effect of tool lead angle and chip formation mode on dust emission in dry cutting. *Journal of Materials Processing Technology*, 194(1-3):100 – 109, 2007. ISSN 0924-0136.

Wohlleben W., Brill S., Meier M. W., Mertler M., Cox G., Hirth S., von Vacano B., Strauss V., Treumann S., Wiench K., Ma-Hock L., and Landsiedel R. On the lifecycle of nanocomposites: Comparing released fragments and their in-vivo hazards from three release mechanisms and four nanocomposites. *Small*, pages 2384–2395, 2011. ISSN 1613-6829.

and Grassian V. H. *Nanoscience and nanotechnology: environmental and health impacts*. John Wiley & Sons, 2008.

W. C. Hinds. *Aerosol Technology: Properties, Behavior, and Measurement of Airborne Particles*. New York:Wiley, 1982.

Vorbau M., Hillemann L., and Stintz M. Method for the characterization of the abrasion induced nanoparticle release into air from surface coatings. *J. Aerosol Sci.*, 40:209–217, 2009.

Leszczynska A., Njuguna J., Pielichowski K., and Banerjee J.R. Thermal stability of polymer/montmorillonite nanocomposites: Part i: Factors influencing thermal stability and mechanisms of thermal stability improvement. *Themochimica Acta*, 453:75–96., 2007a.

Leszczynska A., Njuguna J., Pielichowski K., and Banerjee J.R. Polymer/clay (montmorillonite) nanocomposites with improved thermal properties: Part ii: A review study on thermal stability of montmorillonite nanocomposites based on different polymeric matrixes. *Themochimica Acta*, 454:1–22., 2007b.